Experimental search for the QCD critical endpoint

Ashish Pandav[1,*]

[1]Lawrence Berkeley National Laboratory

Abstract. The phase diagram of strong interaction has been a subject of intense theoretical and experimental research. One of the big questions in this regard is whether a critical endpoint is associated with the phase transition of strongly interacting matter. There have been rapid theoretical developments to answer this question. On the experimental side, a tremendous effort is put forward to hunt for the critical point in collisions of atomic nuclei. This article gives an experimental overview of some of the key results for critical point searches, mainly focusing on net-proton number fluctuations in nuclear collisions.

1 Introduction to experimental search for critical point

The theory governing the strong interaction is the quantum chromo-dynamics (QCD) and its corresponding phase diagram called the QCD phase diagram. A conjectured QCD phase diagram, expressed as a function of temperature (T) vs. baryonic chemical potential (μ_B) is shown as Fig. 1(a). QCD matter with variation in temperature and/or pressure undergoes a phase transition from a chirality asymmetric phase (hadronic) to a phase where chirality is restored (quark-gluon-plasma or the QGP phase). From first-principle lattice-QCD (LQCD) calculations, the nature of this phase transition is established to be a smooth crossover at vanishing μ_B [1]. At large μ_B, theorists resort to effective models or make certain approximations in calculations which suggest of a possible first-order phase transition terminating at the QCD critical point (also called the critical endpoint) [4]. Nonetheless, as seen from Fig. 1(b), the location of the QCD critical point (CP) from various calculations show large variations across the $T-\mu_B$ plane. Therefore, the experimental search for the critical point is extremely important to provide a comprehensive understanding of the QCD phase diagram. Currently, available lattice estimates disfavor critical point for $\mu_B/T < 2$ [2, 3].

The essential idea in the experimental search for CP is to: a) identify CP-sensitive observables, and b) explore its dependence on variation of experimental parameters, such as collision energy of nuclei, its centrality, collision species, and rapidity acceptance of produced particles. The variation of these parameters changes the T and μ_B of the hot and dense system created in nuclear collision [7], thereby allowing access to various regions of the QCD phase diagram. The currently active experiments dedicated to understanding the QCD phase structure are: HADES at SIS18 ($\sqrt{s_{NN}} = 2.4 - 2.7$ GeV), NA61/SHINE at SPS ($\sqrt{s_{NN}} = 5.1 - 17.3$ GeV), STAR at RHIC ($\sqrt{s_{NN}} = 3 - 200$ GeV) and ALICE at LHC ($\sqrt{s_{NN}} = 2.76 - 5.02$ TeV). In regards to the sensitive observables to hunt for CP, there have been several suggestions from theorists. In particular, higher-order cumulants of conserved charges are identified as highly susceptible to the presence of a CP. They are related to the

*e-mail: ashishp.pandav@gmail.com

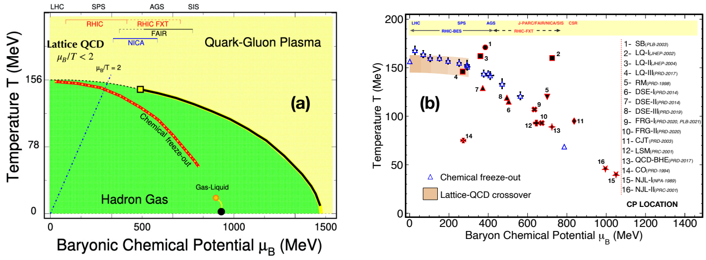

Figure 1. (a) A conjectured QCD phase diagram shown as function of T vs. μ_B. At small μ_B, the dashed line represents the chiral crossover. At large μ_B, the black solid line represents a possible first-order phase transition ending at the critical point (open squared marker). Figure taken from ref.[5]. (b) Theoretical calculations on the location of CP. The abbreviated labels indicate the models and publications (please refer to ref.[6] for details). Figure taken from ref.[6].

correlation length of the system which is known to diverge near a CP [8]. Furthermore, cumulant ratios can be directly related to susceptibility ratios calculated from theory, such as LQCD and thermal models, although there are some caveats. An alternate way to establish the CP is to experimentally validate a crossover at small μ_B and a first-order phase transition at large μ_B and then by thermodynamic arguments, a CP has to exist.

2 Results

This section discusses key results on event-by-event fluctuations of net-proton number (used as a proxy for net-baryon number: a conserved quantity), measured via cumulants (C_n) and their significance in relation to the study of QCD phase transition and critical point.

2.1 Probing thermodynamic equilibrium in nuclear collisions

Thermalization is a crucial step in the formation of QGP and in the study of QCD phase transitions. LQCD calculation ($\mu_B < 110$ MeV), incorporating QCD interactions, suggests of particular ordering of cumulant ratios: $C_3/C_1 > C_4/C_2 > C_5/C_1 > C_6/C_2$, for production of thermalized QCD matter [12]. Figure 2, shows the LQCD calculation along with those from various models at $\sqrt{s_{NN}}$ = 3, 7.7, 39, 200 GeV. The HRG model provides a thermal description of particles produced in heavy-ion collision. However, as seen from the figure, the non-interacting HRG calculations with grand canonical ensemble (GCE) do not show the predicted ordering. Remarkably, with a canonical description of baryon charges in HRG, thereby conserving baryon number exactly, the ordering is observed at all energies from $\sqrt{s_{NN}}$ = 3-200 GeV. On the other hand, the hadronic transport model UrQMD within uncertainties does not show the predicted hierarchy at all energies. Although UrQMD incorporates hadronic interactions, it does not consider thermal equilibrium. It is worth noting from the studies that both features: equilibrium and interaction among the constituents of the system, are needed to observe the aforementioned hierarchy of cumulant ratios. Interesting observations are made when one tests for the ordering in 0-40% central Au+Au collision data from phase I of the Beam Energy Scan program (BES-I) at STAR. Note from Fig. 2, the data within current uncertainties from 7.7 to 200 GeV seem to be consistent with predicted ordering, except at 3 GeV, where a completely reverse trend is seen. The measured trend at 3 GeV is also reproduced by the UrQMD model. This observation could indicate that QCD

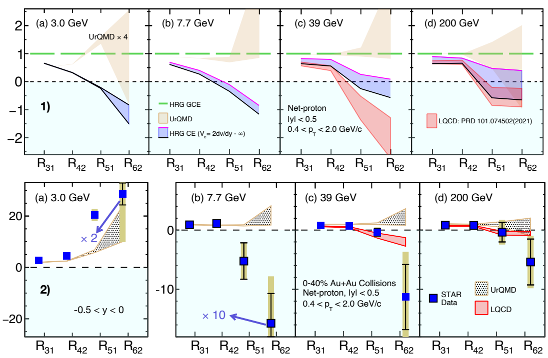

Figure 2. Net-proton cumulant ratios C_3/C_1 (R_{31}), C_4/C_2 (R_{42}), C_5/C_1 (R_{51}), and C_6/C_2 (R_{62}) in Au+Au collisions at $\sqrt{s_{NN}}$ = 3, 7.7, 39, 200 GeV from theory calculations (top 4 panels): UrQMD model (R_{62} at 3 GeV is scaled down by a factor of 4 for better presentation, so the real value sits at the shown value in the figure $\times$ 4) [9], non-interacting HRG with Grand canonical ensemble (HRG GCE), HRG model with canonical treatment for baryon number (HRG CE) [10]. The canonical correlation volume parameter is varied from $V_c = 2$ (black line) $-\infty$ (magenta line). At 3 GeV, only $V_c = 2$ is shown. For $V_c = \infty$, values are taken from ref.[11]. Lattice QCD predictions (only available for $\sqrt{s_{NN}} \geq 39$ GeV) for net-baryon cumulant ratios are shown as red band [12]. Measurements from the STAR experiment at the four collision energies are shown as the blue markers in the bottom 4 panels [9]. The R_{62} data at 3 GeV (7.7 GeV) are scaled down by a factor of 2 (10) for clarity of presentation.

matter falls out of thermal equilibrium at such low collision energies. It is worth mentioning here, that a recent work, requiring a simultaneous description of higher-order fluctuation data in addition to yields in the HRG model with GCE setup, suggests thermalization for $\sqrt{s_{NN}} > 27$ GeV [13].

2.2 Experimental search for a crossover transition

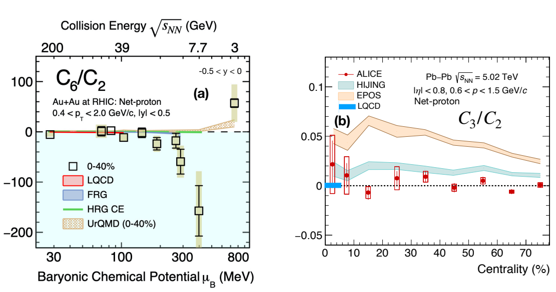

Figure 3. (a) Net-proton C_6/C_2 in 0-40% Au+Au collisions at STAR from $\sqrt{s_{NN}}$ = 3-200 GeV. Also included are various theoretical calculations: LQCD, FRG, HRG CE, and UrQMD. Fig. is taken from Ref. [9]. (b) Net-proton C_3/C_2 from Pb+Pb collisions at $\sqrt{s_{NN}}$ = 5.02 TeV as a function of centrality at ALICE. Fig. is taken from Ref. [14].

A direct experimental verification of crossover transition at small μ_B is facilitated by LQCD. LQCD calculations (μ_B < 110 MeV, equivalently $\sqrt{s_{NN}} \geq 39$ GeV) that include a chiral crossover transition, predict negative signs for fifth and sixth-order net-baryon cumulant ratios near transition temperature [12]. An effective QCD-based model: the functional renormalization group (FRG) also predicts the same sign. The values get progressively negative with decreasing collision energy. Such a trend was indeed observed in the STAR data (see Fig 3. (a)) for sixth-order net-proton cumulant ratio C_6/C_2 for 0-40% centrality over the collision energy range $\sqrt{s_{NN}}$ = 7.7 – 200 GeV, although limited to a significance of $\sim 1.7\sigma$ due to uncertainties [9]. At 3 GeV, the sign turns positive which is reproduced by the hadronic transport model UrQMD. At much large collision energy, such as at $\sqrt{s_{NN}}$ = 5.02 GeV from ALICE ($\mu_B \sim$0), net-proton C_3/C_2 have been reported in Pb+Pb collisions [14] to be consistent with zero and the measurements within uncertainties are consistent with LQCD prediction (see Fig 3. (b)).

2.3 Search for first-order phase transition

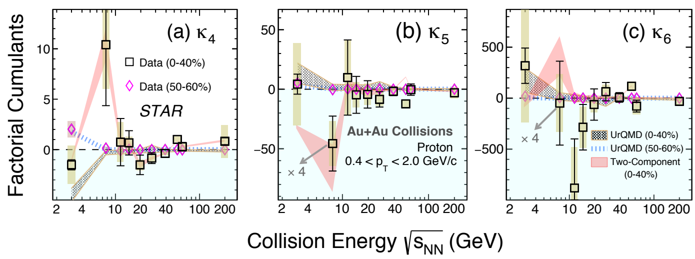

Figure 4. Proton factorial cumulants: κ_4(a), κ_5(b) and κ_6(c) in 0-40% and 50-60% Au+Au collisions. Calculations from the UQMD model and the two-component model are also presented. The κ_5 and κ_6 data at 7.7 GeV (0-40%) are scaled down by a factor of 4 for better illustration. Fig. is taken from [9].

Factorial cumulants (κ_n) of proton multiplicity distribution have been suggested to be sensitive to the presence of a first-order phase transition (FOPT) [15]. The mixed phase in a FOPT is expected to cause a two-component or bimodal shape in the proton multiplicity which leads to large values of higher-order factorial cumulants. The values grow progressively larger with order and flip in sign. The STAR measurements in Au+Au collision from $\sqrt{s_{NN}}$ = 3–200 GeV, and calculations from the UrQMD model and the two-component model that considers measurement up to fourth order as input and then predicts κ_5 and κ_6 are shown in Fig 4. With the given large uncertainties, the comparison of measurements and models indicates the absence of bimodal shape of proton multiplicity distribution for $\sqrt{s_{NN}} \geq 11.5$ GeV that is expected near a FOPT [9].

2.4 Seach for QCD critical point

The STAR experiment observed a non-monotonic collision energy dependence of C_4/C_2 in top 5% Au+Au collisions at a level of $\sim 3\sigma$ over the range $\sqrt{s_{NN}}$ = 7.7 – 62.4 GeV [16](see Fig 5.(a)). Such a trend is consistent with QCD-based model calculation that includes a critical point [8]. Non-critical point models, such as the thermal model HRG and transport model UrQMD fail to explain the observed dependence in the range of 7.7 – 27 GeV. The oscillatory trend in data with respect to models can be seen more clearly from the deviation plot (see Fig 5. (b)) where deviations are observed at a level of $\lesssim 2\sigma$ of the total uncertainties. At 3 GeV, a suppression is observed for C_4/C_2, which is reproduced by UrQMD. Interestingly, the light nuclei compound yield ratio (shown in Fig 5. (c)) also shows deviations from the overall energy dependence trend around 19.6 – 27 GeV [19]. This ratio has been predicted to be sensitive to local density fluctuations near a CP.

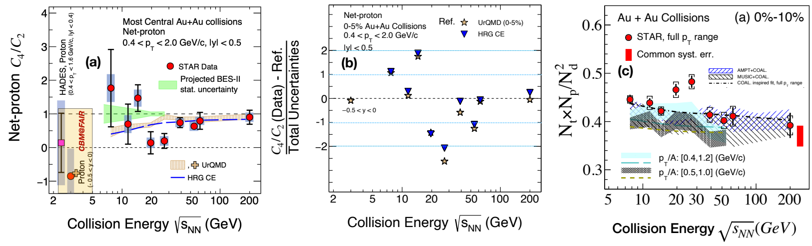

Figure 5. (a) Net-proton C_4/C_2 from STAR in top 5% Au+Au collisions from $\sqrt{s_{NN}} = 3 - 200$ [16, 17] GeV along with HADES data from 0-10% centrality at $\sqrt{s_{NN}} = 2.4$ GeV [18]. Also shown are UrQMD and HRG model calculations with the canonical ensemble. (b) Deviation of C_4/C_2 with respect to model expectations. (c) Light nuclei (proton, deuteron, and triton) yield ratio: $N_t \times N_p/N_d^2$ in top 10% Au+Au collisions from $\sqrt{s_{NN}} = 7.7 - 200$ GeV from STAR. Fig. taken from [19].

3 Conclusions, challenges, and future prospects

The article discussed experimental data on net-proton cumulants in regard to the critical point search. First, a particular ordering of cumulant ratios: $C_3/C_1 > C_4/C_2 > C_5/C_1 > C_6/C_2$ predicted by lattice QCD was studied. It is found from model studies that the observation of this ordering required two features in the system: equilibrium and interaction among constituents of the system. While the STAR measurements in Au+Au collisions from $\sqrt{s_{NN}} = 7.7 - 200$ GeV are generally consistent with this ordering, the data at 3 GeV violates it. This could be suggestive of QCD matter falling out of equilibrium at 3 GeV. Data from STAR and ALICE, especially C_6/C_2 within uncertainties, showed sign and energy dependence trend which is consistent with those from LQCD calculations ($\sqrt{s_{NN}} \geq 39$ GeV) that includes a chiral crossover transition. In the collision energy range, $\sqrt{s_{NN}} = 7.7 - 62.4$ GeV, the net-proton C_4/C_2 exhibits a non-monotonic collision energy dependence, albeit limited to a significance of $\sim 3\sigma$ due to large uncertainties in measurements. It is worth noting that LQCD disfavors a CP for $\mu_B/T < 2$ (corresponds to $\sqrt{s_{NN}} \gtrsim 27$ GeV). The trend and sign of measurements at 3 GeV and their agreement with UrQMD calculation suggest that QCD matter created is hadronic at such low collision energies. This is also supported by the breakdown of the number of constituent quark scaling seen in elliptic flow measurements at 3 GeV [20]. These observations taken collectively indicate that the QCD critical point, if present and if accessible to nuclear collision experiments, is expected within $\sqrt{s_{NN}} = 3 - 27$ GeV.

Model calculation with a CP considering the dynamics of a system created in experiments is currently underway [23] and will be helpful to guide the experimental search for the CP. On the experimental side, the initial volume fluctuation effect remains a challenge to be fully addressed. Since the number of participant nucleons is not directly accessible in experiments, centrality is defined using the produced charged-particle multiplicity. The effect of fluctuation of the number of participants event-by-event on the fluctuations of particle number of interest needs to be fully understood. At high energies, this effect is handled reasonably well using different correction methods [20]. The issue becomes significant at fixed target (FXT) energies, where centrality resolution worsens because of the low charged particle multiplicity produced [17]. While new correction methods are being developed [21], more studies are needed both theoretically and experimentally to understand and control this effect.

The net-proton C_4/C_2 from the STAR BES-I are the first fluctuation measurements exhibiting a non-monotonic energy dependence trend ($\sim 3\sigma$ significance level). However, drawing robust conclusions in relation to CP search would require reducing the uncertainties on net-proton C_4/C_2 considerably. Phase II of the BES program has concluded collecting high statistics Au+Au collision data (factor of 10-20 times larger than in BES-I) from $\sqrt{s_{NN}} = 3-27$ GeV (3-7.7 GeV in FXT mode and 7.7 - 27 GeV in Collider mode). Precision measurements over this range are expected to shed light on the presence of an oscillatory trend in the data. The wider acceptance available due to the iTPC upgrade at BES-II would allow for rapidity dependence studies for fluctuations, which is also beneficial for CP search. However, mid-rapidity proton acceptance at FXT energies ($\sqrt{s_{NN}} \gtrsim 3.9$ GeV) would be challenging at STAR. Fortunately, with the upcoming CBM-FAIR experiment, collection of high statistic Au+Au collisions data ($\sim$ 3 orders of magnitude increase in the interaction rate compared to current experiments) from $\sqrt{s_{NN}} = 2.4-4.9$ GeV with mid-rapidity coverage would be possible. Extending reach to such low energies (high μ_B) would also be important to search for signs of a first-order phase transition. In addition, the 20 billion Au+Au collision events at $\sqrt{s_{NN}} = 200$ GeV to be collected at STAR by 2025 and high statistic LHC Run3 will facilitate the study of a crossover transition in the small μ_B region with C_5 and C_6 measurements.

Acknowledgements*:*

The author thanks the QM2023 IAC and the organizing committee for the invitation to give this talk. Thanks to Drs. X. Dong, B. Mohanty, N. Xu, and the RNC group at LBNL and colleagues from STAR for their valuable inputs. Thanks to Dr V. Vovchenko for helping with the thermal-FIST model. The author acknowledges financial support from DOE, USA.

References

[1] Y. Aoki, *et al.*, Nature **443**, 675-678 (2006)
[2] A. Bazavov, *et al.*, Phys. Rev. D **95**, no.5, 054504 (2017)
[3] S. Borsanyi, *et al.*, Phys. Rev. Lett. **125**, no.5, 052001 (2020)
[4] S. Ejiri, Phys. Rev. D **78**, 074507 (2008)
[5] B. Mohanty and N. Xu, [arXiv:2101.09210 [nucl-ex]].
[6] A. Pandav, D. Mallick and B. Mohanty, Prog. Part. Nucl. Phys. **125**, 103960 (2022)
[7] P. Braun-Munzinger and J. Stachel, Nature **448**, 302 (2007)
[8] M. A. Stephanov, Phys. Rev. Lett. **107**, 052301 (2011)
[9] B. Aboona *et al.* [STAR], Phys. Rev. Lett. **130**, no.8, 082301 (2023)
[10] V. Vovchenko and H. Stoecker, Comput. Phys. Commun. **244**, 295-310 (2019)
[11] P. Braun-Munzinger, *et al.*, Nucl. Phys. A **1008**, 122141 (2021)
[12] A. Bazavov, *et al.*, Phys. Rev. D **101**, no.7, 074502 (2020)
[13] S. Gupta, *et al.*, Phys. Lett. B **829**, 137021 (2022)
[14] S. Acharya *et al.* [ALICE], Phys. Lett. B **844**, 137545 (2023)
[15] A. Bzdak and V. Koch, Phys. Rev. C **100**, no.5, 051902 (2019)
[16] J. Adam *et al.* [STAR], Phys. Rev. Lett. **126**, no.9, 092301 (2021)
[17] M. S. Abdallah *et al.* [STAR], Phys. Rev. Lett. **128**, no.20, 202303 (2022)
[18] J. Adamczewski-Musch *et al.* [HADES], Phys. Rev. C **102**, no.2, 024914 (2020)
[19] M. Abdulhamid *et al.* [STAR], Phys. Rev. Lett. **130**, 202301 (2023)
[20] M. S. Abdallah *et al.* [STAR], Phys. Lett. B **827**, 137003 (2022)
[21] A. Rustamov, J. Stroth and R. Holzmann, Nucl. Phys. A **1034**, 122641 (2023)
[22] M. Abdallah *et al.* [STAR], Phys. Rev. C **104**, no.2, 024902 (2021)
[23] X. An, *et al.* Nucl. Phys. A **1017**, 122343 (2022)